Soft Matter

REVIEW

View Article Online
View Journal | View Issue

Cite this: *Soft Matter*, 2018, **14**, 6949

Structure and behaviour of vesicles in the presence of colloidal particles

Ross W. Jaggers and Stefan A. F. Bon *

Received 14th June 2018,
Accepted 6th August 2018

DOI: 10.1039/c8sm01223g

rsc.li/soft-matter-journal

This review highlights recent studies that investigate the structural changes and behaviour of synthetic vesicles when they are exposed to colloidal particles. We will show examples to demonstrate the power of combining particles and vesicles in generating exciting supracolloidal structures. These suprastructures have a wide range of often responsive behaviours that take advantage of both the mechanical and morphological support provided by the vesicles and the associated particles with preset functionality. This review includes applications spanning a variety of disciplines, including chemistry, biology, physics and medicine.

Vesicles are microscopic sacs dispersed in a liquid medium that enclose finite volumes of the liquid, thereby compartmentalising it from the bulk phase by a thin membrane. They typically form through self-assembly of molecular and/or colloidal building blocks into uni- or multi-lamellar membrane structures. In nature the formation of these vesicular structures forms the basis of protocells, a concept that is considered to be the stepping stone to the origin of life and the predecessor to modern cells.[1–4]

The membranes of naturally occurring vesicles, often referred to as liposomes, and cells are composed of phospholipid amphiphiles. These molecular amphiphiles contain both hydrophilic and hydrophobic domains which allows them to be assembled into bilayer-type or multi-layer hollow structures.[5] Unilamellar membranes are composed of an inner hydrophobic region surrounded by outer hydrophilic domains that face the inner and outer aqueous environments in which the vesicle can be found.[6]

Vesicle formation is driven by the specific amphiphilic architecture of the building blocks expressed by the so-called packing parameter,[7] such that self-assembly spontaneously occurs under appropriate solvent conditions, given that the ratio between the hydrophilic and hydrophobic domains is appropriate.[8–10] The building blocks all have amphiphilic character but can vary in their nature. Copolymers can be used to fabricate polymer vesicles or polymersomes,[11] and Janus particles can be used to build supracolloidal vesicles.[12,13]

Several reviews consider the development and importance of vesicles made from molecules, and the reader is referred to these sources for further information.[6,14–17] This review will take a look at a range of functions that particles can bring to

BonLab, Department of Chemistry, University of Warwick, Coventry, CV4 7AL, UK. E-mail: S.Bon@warwick.ac.uk; Web: www.bonlab.info

Ross Jaggers

Ross Jaggers is a Postdoctoral Research Fellow in the BonLab at the University of Warwick (UK), having completed his PhD under the supervision of Professor Bon from 2013 to 2017. Ross obtained his Masters in Chemistry from the University of York (UK), where he also completed a year in industry at the global Health and Materials Company, DSM, in the Netherlands.

Stefan A. F. Bon

Stefan A. F. Bon is a professor of Chemical Engineering at the University of Warwick (UK). He obtained his PhD from Eindhoven University of Technology (NL) in 1998. He has a background in the mechanistic aspects of free and reversible deactivation radical polymerizations, and is widely regarded as an expert in polymer colloids, especially in the area of emulsion polymerization. In the BonLab (www.bonlab.info) polymer and colloid chemistry is combined with soft matter physics. A chemical engineering twist is added to innovate in supracolloidal materials.

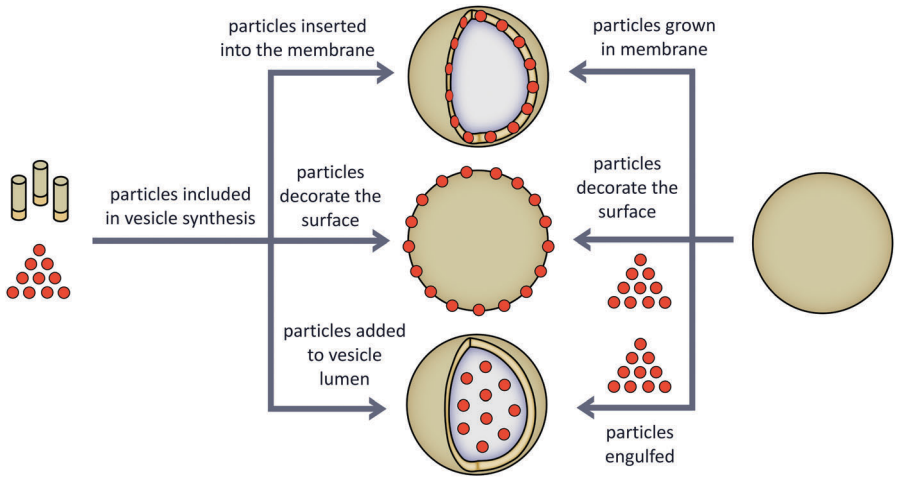

Fig. 1 The various routes towards particle–vesicle composite structures. Particles can be included in the vesicle synthesis to generate vesicles containing particles in their walls, on their surfaces or inside of their lumens (the vesicle core). Alternatively, the particles can be added to pre-formed vesicles to generate the same three structures.

vesicles constructed from molecules, considering the interactions between the two building blocks and the new behaviours that can be derived from the pairing of the two (the possibilities of which are summarised in Fig. 1).

Particles, here defined as localised objects smaller than the vesicle with which they are associated, find use in a wide range of applications such as catalysis,[18,19] drug delivery,[20,21] pigments,[22] nanoswimmers[23,24] and rheology modifiers.[25] Particles can be immobilised within a passive support such as a vesicle, as part of their walls, on their surface, or inside their core. This pairing allows for new hybrid behaviours that neither the particle nor vesicle can exhibit alone.

At over a hundred publications to date, particles and vesicles have been combined in a plethora of ways, tackling a wide range of chemical, biological and physical problems. This review will assess the importance and novelty of a number of examples with a selection of different applications.

The beginnings of composite vesicles: functional liposomes

Artificial liposomes were first synthesised in 1963 by Bangham,[26] but the first mention of combining particles with vesicles was not reported until 1978 by Williams *et al.*[27] In this work, cobalt sulfide particles are grown inside of 25 nm (unless otherwise stated, all vesicle and particle measurements are in diameters) phosphatidylcholine vesicles and used as inorganic probes to track the vesicle. The following year, similar experiments demonstrated the inclusion of magnetite (Fe_3O_4) into these vesicles, however these particles were grown prior to vesicle formation.[28] Due to the limitations of microscopy technology, the precise location of magnetite particles is unknown, however this experiment is the first example of particles being included in a man-made vesicle synthesis. Even as early as 1979, the authors recognised the potential use of these vesicles as magnetic drug carriers. In 1983,[29] Margolis *et al.* demonstrated the association of 50 nm ferromagnetic ferrite particles with liposomes bearing anti-fibronectin antibodies capable of binding to mouse embryo fibroblasts. Upon binding the so called magneto-liposomes, the cells could be sorted using a magnetic field. This study demonstrates how combining the behaviour of a biologically interfacing vesicle with that of functional nanoparticles can generate a new material.

In the same year, Hong *et al.* showed that gold nanoparticles could be internalised within liposomes, where 15 nm gold particles were used as a histological marker to track the uptake and endocytosis of liposomes into cells.[30] Gold nanoparticles are particularly useful in electron as well as dark field light microscopy due to their high electron density, scattering efficiency, size and shape uniformity. Colloidal iron (1–5 nm particles) was later used by Mezei *et al.* for the same reasons to monitor liposome–cell interactions.[31]

These early studies focused on combining the capabilities of particles and vesicles to tackle specific, biological problems. Though several authors published similar studies around this period,[32–34] such as the growth of silver oxide crystals in vesicles[35] or the growth of cadmium sulfide particles in and on vesicles,[36,37] their characterisation of the new composite structures was still limited.

With the advent of vesicles formed from synthetic block-copolymers in 1995 by Eisenberg *et al.*,[11] coined polymersomes in 1999,[14] came more robust synthetic vesicles capable of more severe modifications to their structures.[6] This, along with advancements in electron microscopy (higher resolution and cryogenic techniques, for example) resulted in a number of composite vesicles with a range of new functions and behaviours that could be properly characterised.

In this review, we focus on four ways that particles are able to change the behaviour of lipid or polymer vesicles, namely: the stabilisation of vesicles by particles, shape changes in vesicles, the moderation of membrane permeability, and the taxis of vesicles using particles.

Stabilisation of vesicles by particles

As vesicles are composed of fluid bilayers, they can become colloidally unstable and have a tendency to flocculate and fuse with one another.[38,39] Traditionally, vesicles can be stabilised to protect against exposure to electrolytes by incorporating polyethylene glycol modified lipids into their membranes,[40–42] or by adsorbing polyelectrolytes onto their surfaces,[43,44] to provide steric stabilisation. To reinforce a vesicle membrane and protect it against coalescence, colloidal particles can also be employed to adsorb onto and decorate vesicle surfaces,[45–50] providing stabilisation in the form of an extra barrier. These particles can be polymer latexes,[51–53] silica,[54,55] gold[56] and even hydrogel particles.[57] As always, nature has led the way. For example, bacteria can coat themselves with S-layer proteins,[58] and coccolithophorids (a eukaryotic phytoplankton) have a $CaCO_3$-based nano-patterned colloidal armour.[59]

Back in 1999, Weitz *et al.* demonstrated that arrays of negatively charged microspheres could be assembled onto the outside of positively charged mixed bilayer vesicles, thus forming two-dimensional crystals in adhesive zones of the vesicle only.[60,61]

Zhang *et al.* later showed that if carboxyl modified gold nanoparticles are adsorbed to the outer surface of phospholipid liposomes they can control their fusion activity.[56] As shown in Fig. 2, 4 nm gold nanoparticles are bound to the surface of 1,2-dioleoyl-3-trimethylammonium-propane (DOTAP) vesicles at neutral pH. Liposomes are stabilised whilst the pH is above the pK_a (≈ 5) of the gold's surface carboxylic acid groups ($Au\text{-}COO^-$), but below it, the nanoparticles are protonated (Au-COOH), causing them to detach from the liposome. The subsequent destabilisation of liposomes causes them to fuse with one another. This is interesting because the concept of acid-responsive vesicles could be of use in transdermal drug delivery, as human skin is acidic, especially when infected.[62] One can imagine vesicles that are triggered to fuse and release their contents when in contact with such an acidic surface, delivering medicinal or therapeutic payloads.

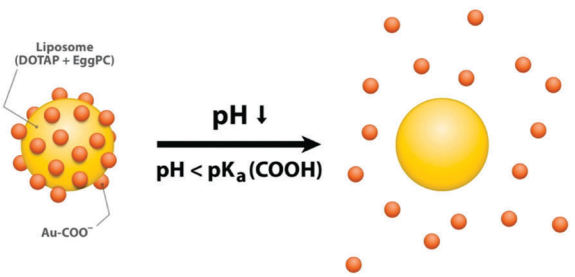

Fig. 2 Schematic illustrations of a carboxyl-modified gold nanoparticle (AuC)-stabilised liposome and its destabilisation at acidic pH. The liposome is stabilised by deprotonated gold particles ($Au\text{-}COO^-$) at neutral pH. When the pH drops below the pK_a value of the carboxylic group (pK_a = *ca.* 5), $Au\text{-}COO^-$ nanoparticles are protonated to form Au-COOH, which subsequently detach from the liposome, resulting in the formation of a bare liposome with fusion activity resuming. Reprinted with permission from D. Pornpattananangkul, S. Olson, S. Aryal, M. Sartor, C.-M. Huang, K. Vecchio and L. Zhang, *ACS Nano*, 2010, **4**, 1935–1942. Copyright 2018 American Chemical Society.[56]

In 2011, we demonstrated versatility in the assembly of polymer latex particles and silica nanoparticles onto the surface of poly(*n*-butyl methacrylate)-*b*-(*N*,*N*-dimethylaminoethyl methacrylate) vesicles, to produce colloidal armours that we observed with cryogenic scanning electron microscopy.[45] We showed the occurrence of a 2D colloidal crystalline armour on the polymersome surface, as well as vesicle surface confined film-formation of soft latex particles and hydrogel formation of a responsive alkali soluble emulsion (ASE) latex.

A further notable example comes from Gradzielski *et al.*, who showed that below their glass transition temperature, 100 nm zwitterionic dipalmitoylphosphatidylcholine (DPPC) lipid vesicles can be effectively stabilised by negatively charged silica nanoparticles.[55] This study is particularly interesting because particle concentration appears to play a key role in determining vesicle stability. Small amounts of surface-adsorbed silica nanoparticles, in this case 16 nm Ludox® HS 40, initially lead to enhanced flocculation, whilst higher concentrations make the vesicles more negatively charged and stable for a longer period of time. This stability is shown to be optimum at neutral pH and at a low ionic strength. The reason why a low particle concentration induces flocculation is somewhat unclear, however the authors speculate that at low concentrations, particles bridge between vesicles, causing them to be brought into close contact whilst still in an unstable state.

Interestingly, local membrane bending is observed where nanoparticles adsorb. As silica particles are adhered to the vesicle membrane below the phase transition temperature of DPPC, indents are made and appear to be retained in the cooling process.

A beautiful example of an entirely soft composite system comes from Nylander *et al.*, who showed that 1,2-dioleoyl-*sn*-*glycero*-3-phosphocholine (DOPC) vesicles can be stabilised by thermoresponsive poly(*N*-isopropylacrylamide) (PNIPAM) particles, as shown in Fig. 3.[57] Responsive polymers that undergo volume phase transitions can be particularly useful as building blocks for self-assemblies,[63,64] as they can adapt their conformation and interactions to their environments.[65–70] Just like their solid-core counterparts, cross-linked polymer particles can act as

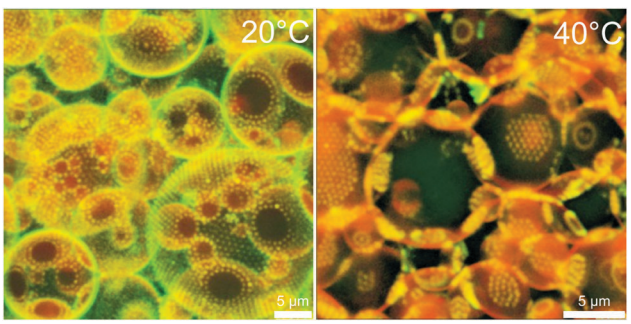

Fig. 3 Fluorescence confocal micrographs of giant lipid vesicles decorated with thermoresponsive PNIPAM microgels at 20 °C (left) and above the PNIPAM volume phase temperature transition at 40 °C (right). Figure is included with permission from A. M. Mihut, A. P. Dabkowska, J. J. Crassous, P. Schurtenberger and T. Nylander, *ACS Nano*, 2013, **7**, 10752–10763; Copyright 2018 American Chemical Society.[57] The original figure is available under the terms of the ACS AuthorChoice license.

Pickering stabilisers at interfaces,[71,72] and PNIPAM particles are no exception. As these microgel particles exhibit a reversible volume phase transition in water around 32 °C, their stabilising efficiency can be controlled as a function of temperature. Below their phase transition the particles stabilise DOPC vesicles, as they behave as soft particles with a 'fuzzy' surface. They adsorb onto the vesicle surface forming densely packed 2D hexagonal arrays across the surface. Above the phase transition temperature, the particles contract into hard spheres, altering the vesicle membrane-microgel interactions and causing microgels to instead rearrange into domains at the vesicle interface (similar to the aforementioned two-dimensional crystal formed on vesicle surfaces by Weitz *et al.*). The authors propose that this is because the microgel particles become smaller, harder, and more hydrophobic, thus creating depletion zones. This demonstrates that the softness and deformability of the particles is crucial for interactions between the particles and the membrane. Again, stabilisation by particles prevents fusion of the vesicles and offers a trigger that could be used in the delivery of active agents by means of temperature change induced vesicle rupture.

Shape changes in vesicles

In these examples of vesicle stabilisation by particles, we have neglected to consider the physical relationship between a hard sphere and a soft elastic membrane.[73] When a particle interacts with a vesicle membrane, whether that be on the inner or outer surface, it can deform the vesicle to induce a range of interesting shape changes. Both local deformation of the membrane by a single particle and the impact on vesicle shape by particles collectively has been studied experimentally[55,74–77] and theoretically.[78–83]

Lecommandoux *et al.* directly observed incorporation of particles in the vesicle membrane,[84–86] when 7.6 nm magnetite nanoparticles were loaded into the walls of amphiphilic polybutadiene-*block*-poly(glutamic acid) di-block copolymer vesicles, either 208 or 624 nm in diameter. The application of a magnetic field allows the shape of the vesicle to be modified, even at relatively low magnetic field intensities (B = 290 G), as shown in Fig. 4.

Instead of embedding particles into the membrane walls, they can be loaded into the lumen (interior) of the vesicle in order to manipulate its structure, as demonstrated by Orwar *et al.*[87] As Fig. 5 shows, 20 nm CdSe/CdTe (core/shell) nanocrystals

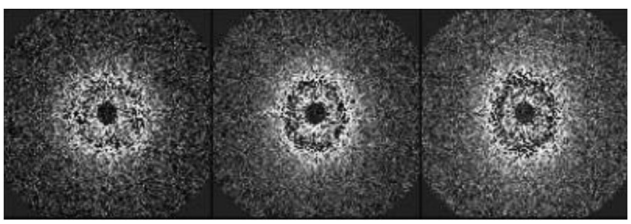

Fig. 4 Deformation of the hollow magnetic shells of vesicles proven by the anisotropy of the 2D SANS patterns under a horizontal magnetic field of intensity B = 0 G (left), B = 540 G (middle) and B = 1050 G (right). Reproduced with permission from Lecommandoux *et al.* Copyright © 2018 Wiley-VCH Verlag GmbH & Co. KGaA, Weinheim.[84]

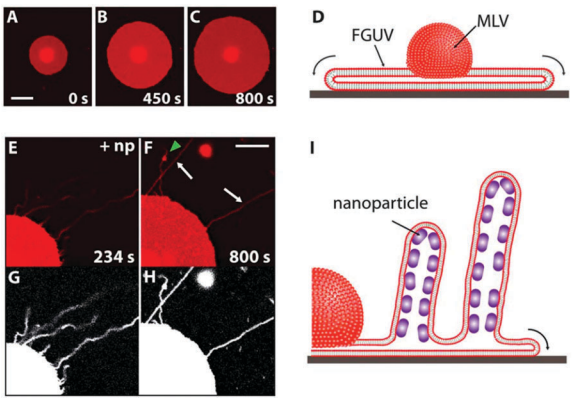

Fig. 5 Spreading and transient tubulation in flat giant unilamellar vesicles (FGUVs) in a 2 mmol dm^{-3} Ca^{2+} containing buffer solution. (A–C) Fluorescence micrograph time series of a FGUV which does not contain nanoparticles and spreads circularly on SiO_2. Scale bar: 20 μm. (D) Schematic drawing of the profile of the FGUV in (A–C) spreading out the lipid material from the multilamellar vesicles (MLV) onto the solid support. Arrows indicate the motion of the rolling bilayer. (E) Fluorescence micrograph of the spreading edge of a nanoparticle encapsulating FGUV, which is displaying transient tubulation while circularly spreading on SiO_2. (F) Fluorescence micrograph of the FGUV at 800 s, when the tubes had retracted into the FGUV. The remaining tubes in (F) became immobilised onto the surface. The green arrow in (F) shows the immobilized end of one tube. Scale bar: 40 μm. (G and H) False colored black and white images of (E and F). (I) Schematic drawing showing the profile of the FGUV in (E–H). Structures in the tubes represent the nanoparticles (20 nm in diameter). Arrow indicates the motion of the rolling bilayer. Reproduced with permission from Orwar *et al.*[87]

can induce tubulation of flat giant unilamellar vesicles (FGUVs) formed from the spreading of *ca.* 20 μm multilamellar soybean lipid vesicles. By encapsulating these particles inside of the vesicle and introducing low concentrations of calcium ions (1–4 mmol dm^{-3}), transient tubes several hundred micrometres in length were formed, analogous to biological nanotubes that fulfil important functions within cells (such as signalling and transport). The authors theorised that these tubes form because of a mismatch between the inner and the outer monolayers of the upper FGUV bilayer, resulting in spontaneous curvature changes.

In contrast, Imai *et al.* confined charged colloidal particles into non-spherical vesicles at much higher volume fractions ($\approx$0.5), transforming them into multi-bead vesicles upon an osmotic pressure difference, as shown in Fig. 6.[88] As the vesicle volume is reduced due to loss of water, preservation of surface area results in an increase in excess area. This excess area leads to non-spherical shapes such as tubes, discocytes or stomatocytes. Packing of particles inside the vesicles transforms them into multi-bead vesicles, in order to obtain the largest free volume for the encapsulated colloids. In considering the shape deformation pathways of these vesicles, the authors theorise that the repulsive interaction between colloids might induce the observed transitions.

Angelani *et al.* theorised that filling vesicles with active particles can also lead to interesting behaviours, as shown in Fig. 7.[89] In their computational study, swimming particles accumulate leading to pinched spots of high density, curvature and pressure. Local fluctuations of particle density produce a

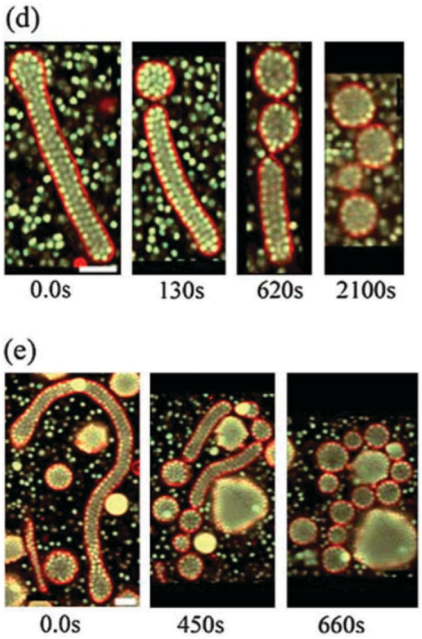

Fig. 6 Shape deformation pathways of giant vesicles encapsulating dense colloids upon the application of an osmotic pressure difference, in the case of (d) medium and (e) long tubes. Reproduced with permission from Imai *et al.*[88]

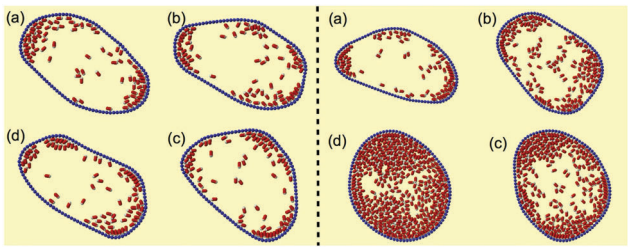

Fig. 7 Shape fluctuations of vesicles where the bounding membrane is composed of N_b = 100 beads, and the vesicle contains active swimmers. Left panel: Snapshots of vesicle shapes explored by the active vesicle for low packing fraction of elongated swimmers (φ = 0.16). Right panel: The vesicle becomes more symmetric as the number of active particles increases, φ is 0.16 (a), 0.31 (b), 0.51 (c) and 0.76 (d). Figure by Angelani *et al.*, reproduced under an Attribution 4.0 International (CC BY 4.0) creative commons licence.[89]

local pressure increase that induces a larger curvature on the flexible membrane. Since active particles tend to accumulate at concave boundaries, this local curvature increase drives further accumulation of swimmers, which in turn raises the local pressure. When vesicle packing is sufficiently high, however, the particles cover the inner membrane uniformly, leading to more consistent pressure and curvature.

Conversely, particles sitting on the surface of vesicles can also induce radical shape changes, as shown in Fig. 8. Safinya *et al.* showed that particles can induce pinched shape deformations of the membrane of a vesicle, and, if a number of particles are decorating a fluid membrane, they can interact with one another.[90] Giant unilamellar 1-palmitoyl-2-oleoyl phosphocholine and dimiristoyl phosphocholine liposomes (10 μm) were decorated

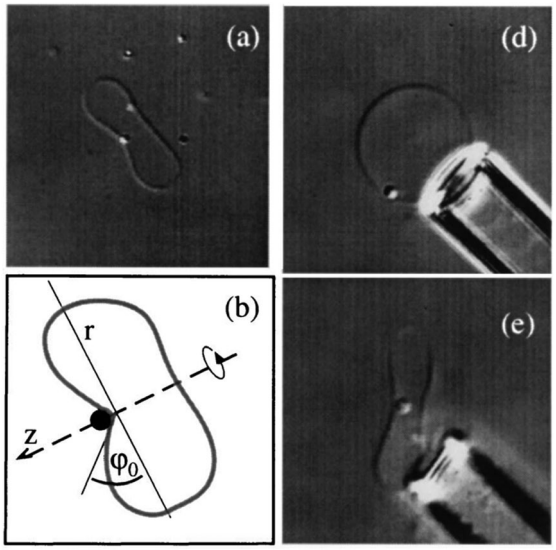

Fig. 8 (a) A giant liposome with a single 0.9 μm bead attached to it. (b) Schematic of a pinched, hat like membrane deformation around a bead, observed practically with a single bead on a vesicle. (d) A bead on a vesicle held still by a suction pipette. (e) The same bead and vesicle after release from the pipette tip. Reprinted (Fig. 1) with permission from I. Koltover, J. O. Rädler and C. R. Safinya, *Phys. Rev. Lett.*, 82, 1991–1994, 1999. Copyright 2018 by the American Physical Society.[90]

with protein grafted latex beads (0.9 μm). Vesicles with single beads attached clearly show induced contours around the bound bead, and interestingly, particles appear to be driven to negative curvature regions on non-spherical vesicles, the most energetically favoured conformation. When two beads are attached to spherical vesicles, there is no preferential location and the beads approach each other if lipid mobility is preserved (*i.e.* above the lipid chain melting temperature). Critically, the beads do not aggregate freely in solution, thus their approach is not mediated by colloidal interactions alone. This collective particle behaviour can even generate ring shaped strings of beads around the waist of a dumbbell shaped vesicle, notable as the precursor to the budding and fission of membranes.

A vesicle's lipid bilayer provides resistance against bending, such that there is an associated bending energy upon deformation of the vesicle membrane. Bending forces are particularly important for modelling biological vesicles, red blood cells and capsules.[91] They are typically calculated from an energy function based on the bending energy density for a given membrane geometry, where the local bending energy density is proportional to the square of the local surface curvature.[92] This bending energy has been quantified in different ways by authors such as Canham,[93] Evans,[94] and Weiner,[95] where all models depend on the square of the mean curvature, but the most commonly used model for calculating the energy per unit deformed area is that of Helfrich.[96,97] The Helfrich Curvature Free Energy can be used to qualitatively understand the relative stability of different bilayer structures. A preferred vesicle shape arises from competition between curvature energy (deriving from membrane bending elasticity), geometrical constraints such as fixed surface area and enclosed volume, and the specific bilayer aspect.[98]

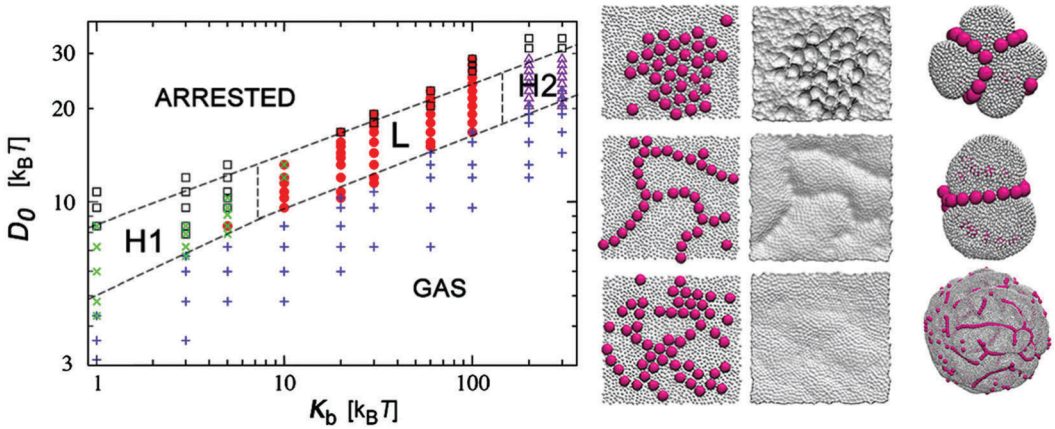

Fig. 9 Left panel: Phase diagram of particle self-assembly on a fluid surface in terms of the surface bending rigidity k_b and particle binding energy D_0. Middle panel: The snapshots show typical aggregates in the H_1, L, and H_2 phases in a top-to-bottom order and the deformation pattern they leave on the membrane. The membrane area is $A \approx (40 \times 40)\sigma^2$, the nanoparticle size $\sigma_{np} = 4\sigma$, and their surface fraction $\rho = 0.27$. Right panel: Snapshots of the linear aggregates on the spherical membrane. Reproduced with permission from Safinya *et al.* Reprinted (Fig. 1) with permission from A. Šarić and A. Cacciuto, *Phys. Rev. Lett.*, **108**, 118101, 2012. Copyright 2018 by the American Physical Society.[99]

Sticking with the interaction of multiple beads on a vesicle surface, Cacciuto and Šarić computed a phase diagram for the different aggregates formed by nanoparticles adsorbing onto a lipid bilayer as a function of surface bending rigidity and nanoparticle adhesive energy, as shown in Fig. 9.[99] Over a wide range of bending rigidities ($\approx$10–100 k_BT), nanoparticles can organise into linear aggregates, providing that the binding energy is sufficiently large. Similar to the experimental observations of Safinya *et al.*, particles can pinch around the circumference of a vesicle, this time into longer chains.

Finally, vesicles can engulf particles that adhere to their surfaces in a similar fashion to cellular uptake, termed endocytosis. During endocytosis, molecules adhere to the membrane, the bilayer invaginates and the target is completely wrapped in a newly formed vesicle.[100]

Several studies consider this process both theoretically and experimentally,[101–110] but we will focus on two noteworthy examples. The first from Kroeger *et al.* presents experimental evidence of the internalisation of particles by 110 nm poly(dimethylsiloxane)-*block*-poly(2-methyloxazoline) vesicles.[105] Using photon- and fluorescence-correlation spectroscopy, the authors show species-selective uptake, dependent on particle size and concentration. A threshold concentration for particle uptake is shown, explained by the surface area ratio between polymersomes and particles necessary for successful particle adhesion to the membrane. Unsurprisingly, a higher concentration of nanoparticles leads to internalisation of more particles. Furthermore, size selectivity is seen. Loading incorporation rates decrease as the nanoparticle radius increases from 15, to 36 to 57 nm, but interestingly, cryo-TEM reveals that particles are engulfed *via* different mechanisms depending on their size. Smaller particles are engulfed as clusters instead of single wrapped particles, as in the case of larger nanoparticles.

The phenomenon of particle endocytosis by vesicles was also approached from a theoretical standpoint by Gao and Yi, where they consider the effects of particle size and elasticity on particle incorporation.[111] In this study, elastic particles of different sizes and rigidities are incorporated into a lipid vesicle of fixed surface area, whilst the size of the particle determines the mode of particle uptake. The incorporation of small particles leads to continuous vesicle volume evolution, as the vesicle undergoes a smooth shape transformation. Conversely, vesicles wrapping a large particle undergo a discontinuous shape transition from concave shallow bowl-shaped stomatocytes into closed cups. Furthermore, softer particles are more prone to partial wrapping but require stronger adhesion energy to be fully engulfed. By taking into consideration adhesion energy, size, and rigidity ratios between particles and vesicles, as well as the spontaneous curvature of the vesicle, the authors construct wrapping phase diagrams containing all wrapping states.

Moderating membrane permeability

Vesicle membranes are self-assembled bilayers of amphiphiles, and as such have a characteristic fluidity (as the term fluid mosaic model describing a cell membrane devised in 1972 suggests).[112] This fluidity allows for ions and small molecules to pass through the membrane and makes vesicles inherently leaky, and thus an increase in membrane fluidity results in an increase in membrane permeability.

In 2016, we showed that embedding manganese oxide (MnO_2, *ca.* 3 μm) nanoparticles into the walls of multilamellar polymer vesicles allows for the spatial and temporal regulation of membrane permeability by the introduction of a chemical trigger (see Fig. 10).[113] 300 μm MnO_2 embedded poly(butyl methacrylate)-*block*-poly(dimethylaminoethyl methacrylate) vesicles were synthesised using flow-focused microfluidics. Upon exposure to low concentrations of hydrogen peroxide, an enhancement in the rate of release of vesicle contents is observed, whereas a high concentration causes vesicle rupture and complete release. We hypothesise that the increase in release is due to an increase in

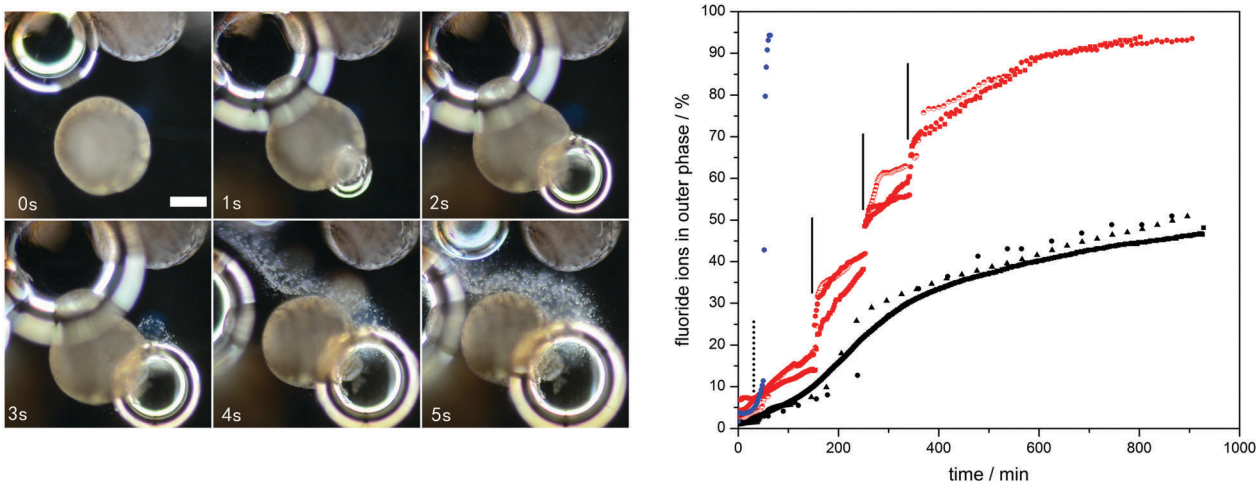

Fig. 10 Left: Dark microscopy sequence of video stills of a dispersion of vesicles in $Ba^{2+}_{(aq)}$ with membrane embedded manganese oxide particles, loaded with sodium sulfate, after the addition of a large aliquot of hydrogen peroxide. The stills show the formation of oxygen bubbles, leading to deformation and rupture of the vesicle membranes thereby releasing the sulfate ion content, as visualised by the formation of a stream of *in situ* formed barium sulfate particles (a white haze). Scale bar: 150 μm. Right: Fluoride ion release profiles of water-based dispersions of *ca.* 6000 MnO_2 particle embedded vesicles containing 0.2 mol dm^{-3} sodium fluoride (6 cm^3 of water outer phase, 0.1 cm^3 of inner aqueous phase) with (a) 3.0 cm^3 of 30 wt% H_2O_2 added at 50 min (blue, dashed vertical line indicates time of hydrogen peroxide addition), (b) aliquots of 0.2 cm^3 of 3 wt% H_2O_2 added at 150, 250 and 340 min (red, solid vertical lines indicate time of hydrogen peroxide addition), and (c) no H_2O_2 stimulus (black). Reproduced with permission from Bon *et al.*[113]

vesicle permeability caused by the catalytic activity of the particles, likely due to the generation of oxygen bubbles. This work is an example of chemically regulated membrane permeability and offers an alternative to more traditional methods of regulation, such as membrane proteins or the other external triggers previously discussed.[16]

Paasonen *et al.* show that heating gold nanoparticles can also be an effective way to increase membrane fluidity.[114] 200–500 nm DPPC and distearoylphosphatidylcholine (90 : 10) liposomes were loaded with 1.4 nm gold nanoparticles and exposed to 250 nm UV light. Irradiation causes local heating of the particles so they act as localised heat sources, absorbing UV radiation and transferring heat to the membrane. The authors hypothesise that the permeability of the bilayer is increased by the separation of gel and fluid phases, allowing the encapsulated dye calcein to escape. Interestingly, triggered release of the dye was observed when gold particles are on the outer and inner membrane, as well as when part of the membrane itself.

Amphiphiles can be assembled into giant unilamellar vesicles (GUVs) and multilamellar vesicles with diameters of 1–500 μm using microfluidic templating,[115] to generate a wide range of fascinating structures.[116] For example, Nie *et al.* formed 1.28 μm gold nanorod embedded poly(ethylene oxide)-*block*-polystyrene (PEO-*b*-PS) vesicles from the microfluidic-assisted assembly of PEO-*b*-PS-tethered gold nanorods (40 nm by 10 nm), as shown in Fig. 11.[117] Upon irradiation with near infrared light (700 to 1000 nm), these vesicles can be burst to deliver a payload due to intense localised heating. Laser exposure causes the rods to deform into spherical nanoparticles due to photothermally induced melting, and this shape deformation is theorised to create extra spacing between particles for the release of encapsulated molecules.

Remarkably, nanoparticles need not be embedded in the membrane itself, but can impact fluidity by simply being in close proximity to the vesicle.[118–125] Zasadzinski *et al.* showed that DPPC vesicles either loaded with, covered in, or found near to hollow gold nanoshells (HGNs) could be irradiated with near infrared radiation to achieve near instantaneous release of liposome contents.[120] The laser-heated HGNs act as nanosonicators to temporally disrupt the lipid membrane, but are most effective when tethered to the vesicle surface. The membrane permeabilising power of a gold particle as a function of its distance from the vesicle was further investigated by Oddershede *et al.*, demonstrating the concept of 'controlled leakage' mediated by particle distance, as shown in Fig. 12.[121]

The use of an alternating magnetic field (AMF) has also been shown to trigger release from vesicles containing iron oxide nanoparticles in their walls.[126] When AMF pulses were applied to PEGylated 2-distearoyl-*sn*-*glycero*-3-phosphocholine vesicles containing 5 nm iron oxide particles in their walls, the release rates of the membrane impermeable dye calcein increased. Critically, hyphenating 1 minute AMF pulses with 1 minute equilibrium periods resulted in a more constant release rate than in the case of longer pulsing cycles.

It is not just the magnetic susceptibility of iron oxide that makes it a useful tool in membrane functionalisation. Exposure to radio frequencies causes nanoparticle heating and can lead to increased membrane permeability, as shown by Bothun *et al.* in Fig. 13.[127] 100 nm DPPC vesicles containing 5 nm oleic acid stabilised maghemite particles in their walls (confirmed by cryo-TEM) were loaded with solutions of the fluorescent dye carboxyfluorescein. Dye leakage from the vesicles was significantly increased upon exposure to radio frequency heating at optimum lipid molecule to nanoparticle ratios (5000 : 1, in this study), justified

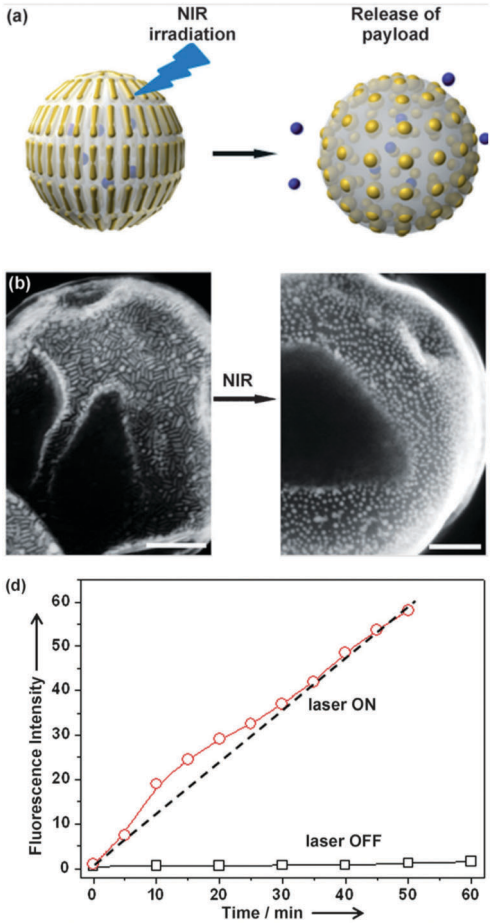

Fig. 11 (a) Near infrared triggered release using giant vesicles. The photothermally induced shape deformation of gold nanorods into spherical nanoparticles creates extra spacing between particles for the release of encapsulated molecules. (b) SEM images of giant vesicles before and after exposure to the laser, showing the shape deformation. Scale bars are 200 nm. (d) The release profiles of Rhodamin B giant vesicles with laser on (○) and laser off (□). Reproduced with permission from Nie *et al.*[117] Copyright © 2018 Wiley-VCH Verlag GmbH & Co. KGaA, Weinheim.

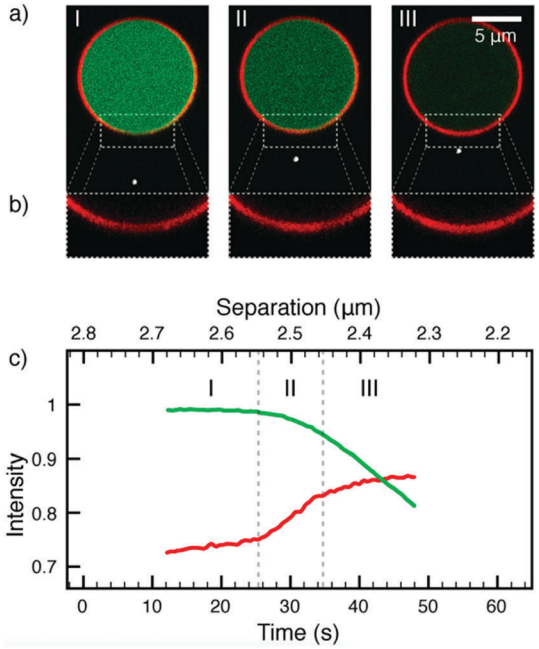

Fig. 12 Controlled leakage of a GUV upon approach of an optically trapped gold nanoparticle. (a) Confocal images of a GUV surface (red), its cargo (green), and an optically trapped gold nanoparticle (bright white spot) as the trapped nanoparticle approaches the GUV. (b) Zoom in on the membrane in the boxes of (a). (c) Intensity of the fluorophores (the alexa hydrazide (AH) and Texas Red) in the boxed regions of (a) as a function of travelled distance. The AH signal is normalized by its initial value, and the intensity of Texas Red is normalised by the initial AH value. The GUV becomes leaky around t = 26 s. Reprinted with permission from A. Kyrsting, P. M. Bendix, D. G. Stamou and L. B. Oddershede, *Nano Lett.*, 2011, **11**, 888–892.[121] Copyright 2018 American Chemical Society.

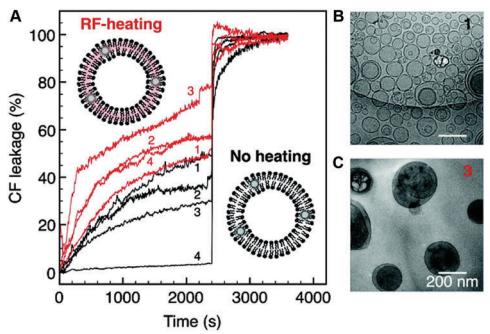

Fig. 13 Carboxyfluorescein (CF) leakage from bilayer decorated magnetic liposomes (dMLs). (A) Percent CF leakage with (red) and without (black) radiofrequency (RF) heating at 250 A and 281 kHz for (1) DPPC and dMLs formed at lipid molecule to nanoparticle (L/N) ratios of (2) 25 000 : 1, (3) 10 000 : 1, and (4) 5000 : 1. The inset schematics (not to scale) in (A) depict dML heating with or without RF heating. Cryo-TEM images are shown at 10 mM lipid for (B) DPPC liposomes and (C) dMLs formed at a L/N ratio of 10 000 : 1 (200 nm scale bars). Reprinted with permission from Y. Chen, A. Bose and G. D. Bothun, *ACS Nano*, 2010, **4**, 3215–3221.[127] Copyright 2018 American Chemical Society.

by a trade-off between structural changes and aggregation that impacts local heating and membrane permeability. The authors rightly consider that the inclusion of particles into membranes is, by design, disruptive to the membrane and can have a negative impact on vesicle stability. As many authors make clear, a balance between structural integrity and particle functionality must be sought, especially when attempting to moderate membrane permeability.[128–130]

These examples show that colloidal metal nanoparticles, specifically iron oxide, gold and silver, can act as effective heat transducers that directly impact the structural integrity of a vesicle membrane. In comparison to bulk heating, these composite systems provide the added benefit of precise spatial and temporal control.

In fact, particles can still change membrane permeability without heating. Oh *et al.* showed that by simply including silver and gold nanoparticles in the walls, DPPC vesicle permeability could be increased.[131,132] By monitoring the movement of dye molecules in the membrane using fluorescent anisotropy spectroscopy, membrane fluidity is measured and shown to be higher for vesicles containing nanoparticles.

Taxis of vesicles using particles

Several of the examples discussed so far have used the release of vesicle contents as a probe for change in membrane structure. There are, however, composite vesicles that have been designed with triggered release as their primary function, capable of some rather unique behaviours.[113,133–142]

Extracellular vesicles form naturally during biological functions for purposes such as storage, transport, and communication,[143] therefore it is not surprising that synthetic vesicles have been designed to carry out similar tasks. One such example is the transport and delivery of a drug by Janus vesicles powered by platinum and gold nanoparticles, as shown in Fig. 14.[133] Vesicles were synthesised from a combination of free PEO-*b*-PS polymer and PEO-*b*-PS polymer tethered nanoparticles that phase separate during synthesis to yield Janus (two-faced) structures. Platinum catalyses the breakdown of hydrogen peroxide into water and oxygen bubbles, providing a source of propulsion when embedded into the walls of a vesicle. As the platinum particles are confined to one side of the vesicle it is propelled with direction, and once it arrives at its destination, a near infra-red laser heats the gold particles in the walls bursting the vesicle and releasing the encapsulated drug.

Swimming, by means of bubble propulsion, is possible whether you are at the nano-[24] or millimetre length scale,[144] and as van Hest and Wilson note, such self-propelling objects are reminiscent of miniature rocket engines, as shown in Fig. 15.[142,145] Their work concerns the propulsion of so called stomatocytes, bowl shaped structures formed by the osmotic deformation of polymer vesicles. The stomatocytes have platinum nanoparticles entrapped within their cavities that, when exposed to hydrogen peroxide fuel, generate a rapid discharge of oxygen bubbles from their opening that induces movement. Their speed is determined not only by the concentration of the fuel in the continuous phase, but also by growing temperature-sensitive polymer brushes onto the motor. These polymer brushes moderate the stomatocyte opening size upon a temperature change; thus the hydrogen peroxide influx can be controlled and the vesicle's speed regulated.

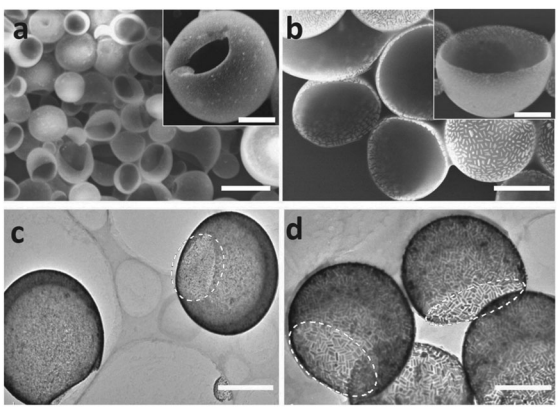

Fig. 14 Top: (a and b) SEM images of vesicles containing block copolymer tethered gold nanorods, showing that the vesicle is hollow. (c and d) TEM images of composite vesicles containing platinum and gold nanoparticle rich domains, identified by the dashed circles. Scale bars are 1 μm in image (c) and 500 nm in image (d). Reproduced with permission from Nie *et al.*[133] Copyright © 2018 Wiley-VCH Verlag GmbH & Co. KGaA, Weinheim.

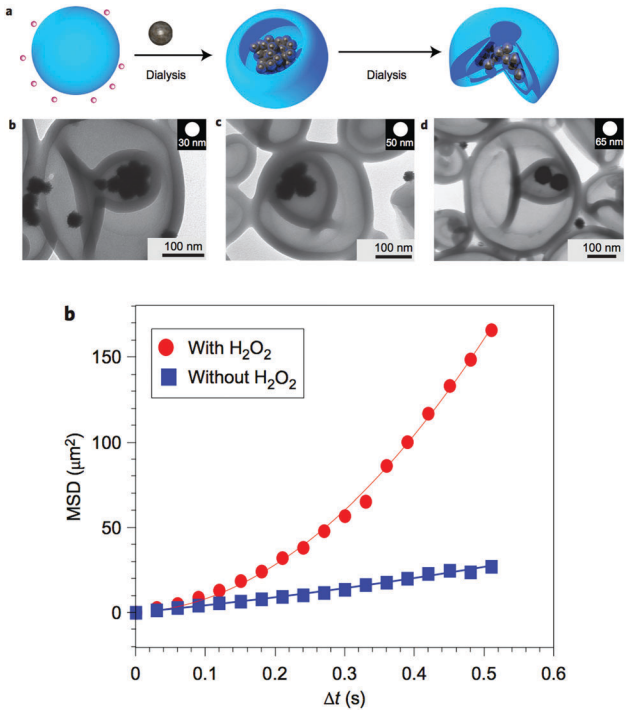

Fig. 15 Top: (a) Strategy for entrapping preformed platinum nanoparticles during the transformation of vesicles into stomatocytes. (b, c and d) show TEM images of entrapped nanoparticles of different sizes (30, 50 and 65 nm, respectively). Bottom: Average mean square displacement (MSD) of the platinum-filled stomatocytes before and after the addition of 20 cm^3 H_2O_2, calculated from the tracking coordinates of 57 particles (the particles were selected from the upper part of the major size distribution). Adapted by permission from Macmillan Publishers Ltd: D. A. Wilson, R. J. M. Nolte and J. C. M. van Hest, *Nat. Chem.*, 2012, **4**, 268–274, copyright 2018.[142]

More recently, Battaglia *et al.* showed that synthetic vesicles could cross the blood–brain barrier by means of chemotactic transport.[146] By fabricating polymersomes from blends of two different copolymers, asymmetric structures are formed. These polymersomes are filled with glucose oxidase that catalyzes the breakdown of glucose to glucono δ-lactone and hydrogen peroxide, and catalase to catalyze the decomposition of hydrogen peroxide into water and oxygen. By forming the vesicle from polymers of different permeabilities, the reaction products are preferentially expelled from one region of the vesicle, thus generating a vesicle capable of directed self-propulsion. These loaded vehicles are able to penetrate the blood–brain barrier four times more effectively than their comparable non-chemotactic systems.

Outlook

In this review, we have shown a number of examples that demonstrate the power of combining particles and vesicles into new and exciting superstructures. These nanocomposites have a wide range of functions and behaviours that take advantage of both the functional support provided by the vesicles and the associated active particles, in most cases yielding responsive entities.

We hope that these experimental and theoretical studies inspire readers to consider the variety and complexity of structures that can be created.

A number of our examples theorise the possibilities for particle–vesicle composites that are yet to be experimentally realised, and one can expect the next decade of research to present a host of new and exciting systems developed across many disciplines. With a wide range of building blocks available, the possibilities for creating novel functional materials are endless, and the reader is encouraged to use their imagination when designing their future composite superstructures.

Conflicts of interest

There are no conflicts to declare.

References

1 G. Wächtershäuser, *Mol. Microbiol.*, 2003, **47**, 13–22.
2 D. A. Hammer and N. P. Kamat, *FEBS Lett.*, 2012, **586**, 2882–2890.
3 J. C. Blain and J. W. Szostak, *Annu. Rev. Biochem.*, 2014, **83**, 615–640.
4 S. S. Mansy and J. W. Szostak, *Proc. Natl. Acad. Sci. U. S. A.*, 2008, **105**, 13351–13355.
5 J. N. Israelachvili, *Intermolecular and surface forces*, Academic Press, Cambridge, MA, 2011.
6 D. E. Discher and A. Eisenberg, *Science*, 2002, **297**, 967–973.
7 J. N. Israelachvili, D. J. Mitchell and B. W. Ninham, *J. Chem. Soc., Faraday Trans. 2*, 1976, **72**, 1525–1568.
8 J. N. Israelachvili, D. J. Mitchell and B. W. Ninham, *Biochim. Biophys. Acta, Biomembr.*, 1977, **470**, 185–201.
9 M. P. Sheetz and S. J. Singer, *Proc. Natl. Acad. Sci. U. S. A.*, 1974, **71**, 4457–4461.
10 J. N. Israelachvili and D. J. Mitchell, *Biochim. Biophys. Acta*, 1975, **389**, 13–19.
11 L. Zhang and A. Eisenberg, *Science*, 1995, **268**, 1728–1731.
12 S. Whitelam and S. A. F. Bon, *J. Chem. Phys.*, 2010, **132**, 074901.
13 G. Avvisati, T. Vissers and M. Dijkstra, *J. Chem. Phys.*, 2015, **142**, 084905.
14 B. M. Discher, Y.-Y. Won, D. S. Ege, J. C.-M. Lee, F. S. Bates, D. E. Discher and D. A. Hammer, *Science*, 1999, **284**, 1143–1146.
15 R. P. Brinkhuis, F. P. J. T. Rutjes and J. C. M. van Hest, *Polym. Chem.*, 2011, **2**, 1449–1462.
16 C. Schmitt, A. H. Lippert, N. Bonakdar, V. Sandoghdar and L. M. Voll, *Front. Bioeng. Biotechnol.*, 2016, **4**, 19.
17 V. P. Torchilin, *Nat. Rev. Drug Discovery*, 2005, **4**, 145–160.
18 P. J. F. Harris, *Int. Mater. Rev.*, 1995, **40**, 97–115.
19 B. Hvolbæk, T. V. W. Janssens, B. S. Clausen, H. Falsig, C. H. Christensen and J. K. Nørskov, *Nano Today*, 2007, **2**, 14–18.
20 W. H. De Jong and P. J. A. Borm, *Int. J. Nanomed.*, 2008, **3**, 133–149.
21 M. Gaumet, A. Vargas, R. Gurny and F. Delie, *Eur. J. Pharm. Biopharm.*, 2008, **69**, 1–9.
22 D. A. Scott, *Stud. Conserv.*, 2016, **61**, 185–202.
23 A. R. Morgan, A. B. Dawson, H. S. Mckenzie, T. S. Skelhon, R. Beanland, H. P. W. Franks and S. A. F. Bon, *Mater. Horiz.*, 2014, **1**, 65–68.
24 B. W. Longbottom, L. A. Rochford, R. Beanland and S. A. F. Bon, *Langmuir*, 2015, **31**, 9017–9025.
25 J. A. Bonham, M. A. Faers and J. S. van Duijneveldt, *Soft Matter*, 2014, **10**, 9384–9398.
26 A. D. Bangham, *Adv. Lipid Res.*, 1963, **1**, 65–104.
27 A. J. Skarnulis, P. J. Strong and R. J. P. Williams, *J. Chem. Soc., Chem. Commun.*, 1978, **0**, 1030–1032.
28 S. Mann, A. J. Skarnulis and R. J. P. Williams, *J. Chem. Soc., Chem. Commun.*, 1979, **0**, 1067–1068.
29 L. B. Margolis, V. A. Namiot and L. M. Kljukin, *Biochim. Biophys. Acta, Biomembr.*, 1983, **735**, 193–195.
30 K. Hong, D. S. Friend, C. G. Glabe and D. Papahadjopoulos, *Biochim. Biophys. Acta, Biomembr.*, 1983, **732**, 320–323.
31 M. Foldvari, G. T. Faulkner and M. Mezei, *J. Microencapsulation*, 1988, **5**, 231–241.
32 K. Gao and L. Huang, *Biochim. Biophys. Acta, Biomembr.*, 1987, **897**, 377–383.
33 P. Herve, F. Nome and J. H. Fendler, *J. Am. Chem. Soc.*, 1984, **106**, 8291–8292.
34 S. Mann and J. P. Hannington, *J. Colloid Interface Sci.*, 1988, **122**, 326–335.
35 J. L. Hutchison, S. Mann, A. J. Skarnulis and R. J. P. Williams, *J. Chem. Soc., Chem. Commun.*, 1980, **0**, 634–635.
36 Y. M. Tricot and J. H. Fendler, *J. Phys. Chem.*, 1986, **90**, 3369–3374.
37 H. J. Watzke and J. H. Fendler, *J. Phys. Chem.*, 1987, **91**, 854–861.
38 E. Evans and M. Metcalfe, *Biophys. J.*, 1984, **46**, 423–426.
39 E. Evans and D. Needham, *J. Phys. Chem.*, 1987, **91**, 4219–4228.
40 S. Rangelov, K. Edwards, M. Almgren and G. Karlsson, *Langmuir*, 2003, **19**, 172–181.
41 D. D. Lasic, *Angew. Chem., Int. Ed. Engl.*, 1994, **33**, 1685–1698.
42 K. Kostarelos, T. F. Tadros and P. F. Luckham, *Langmuir*, 1999, **15**, 369–376.
43 M. M. Mady and M. M. Darwish, *J. Adv. Res.*, 2010, **1**, 187–191.
44 F. Quemeneur, M. Rinaudo, G. Maret and B. Pépin-Donat, *Soft Matter*, 2010, **6**, 4471–4481.
45 R. Chen, D. J. G. Pearce, S. Fortuna, D. L. Cheung and S. A. F. Bon, *J. Am. Chem. Soc.*, 2011, **133**, 2151–2153.
46 X. Chen, G. Zou, Y. Deng and Q. Zhang, *Nanotechnology*, 2008, **19**, 195703.
47 F. De Persiis, C. La Mesa and R. Pons, *Soft Matter*, 2012, **8**, 1361–1368.
48 H. Pera, T. M. Nolte, F. A. M. Leermakers and J. M. Kleijn, *Langmuir*, 2014, **30**, 14581–14590.
49 K. Shigyou, K. H. Nagai and T. Hamada, *Langmuir*, 2016, **32**, 13771–13777.
50 R. Sarfati and E. R. Dufresne, *Phys. Rev. E*, 2016, **94**, 012604.
51 L. Zhang and S. Granick, *Nano Lett.*, 2006, **6**, 694–698.
52 L. Zhang, L. Hong, Y. Yu, S. Chul Bae and S. Granick, *J. Am. Chem. Soc.*, 2006, **128**, 9026–9027.

53 Y. Yu, S. M. Anthony, L. Zhang, S. Chul Bae and S. Granick, *J. Phys. Chem. C*, 2007, **111**, 8233–8236.
54 S. Savarala, S. Ahmed, M. A. Ilies and S. L. Wunder, *ACS Nano*, 2011, **5**, 2619–2628.
55 R. Michel, T. Plostica, L. Abezgauz, D. Danino and M. Gradzielski, *Soft Matter*, 2013, **9**, 4167–4177.
56 D. Pornpattananangkul, S. Olson, S. Aryal, M. Sartor, C.-M. Huang, K. Vecchio and L. Zhang, *ACS Nano*, 2010, **4**, 1935–1942.
57 A. M. Mihut, A. P. Dabkowska, J. J. Crassous, P. Schurtenberger and T. Nylander, *ACS Nano*, 2013, **7**, 10752–10763.
58 M. Sára and U. B. Sleytr, *J. Bacteriol.*, 2000, **182**, 859–868.
59 J. R. Young, S. A. Davis, P. R. Bown and S. Mann, *J. Struct. Biol.*, 1999, **126**, 195–215.
60 H. Aranda-Espinoza, Y. Chen, N. Dan, T. C. Lubensky, P. Nelson, L. Ramos and D. A. Weitz, *Science*, 1999, **285**, 394–397.
61 L. Ramos, T. C. Lubensky, N. Dan, P. Nelson and D. A. Weitz, *Science*, 1999, **286**, 2325–2328.
62 M.-H. Schmid-Wendtner and H. C. Korting, *Skin Pharmacol. Physiol.*, 2006, **19**, 296–302.
63 M. Shibayama and T. Tanaka, *Volume phase transition and related phenomena of polymer gels*, Springer, Berlin Heidelberg, 1993.
64 Y. Li and T. Tanaka, *Annu. Rev. Mater. Sci.*, 1992, **22**, 243–277.
65 Y. Chen, N. Ballard and S. A. F. Bon, *Chem. Commun.*, 2013, **49**, 1524–1526.
66 Y. Chen, N. Ballard and S. A. F. Bon, *Polym. Chem.*, 2013, **4**, 387–392.
67 R. V. Bell, C. C. Parkins, R. A. Young, C. M. Preuss, M. M. Stevens and S. A. F. Bon, *J. Mater. Chem. A*, 2016, **4**, 813–818.
68 Y. Chen, N. Ballard, O. D. Coleman, I. J. Hands-Portman and S. A. F. Bon, *J. Polym. Sci., Part A: Polym. Chem.*, 2014, **52**, 1745–1754.
69 G. Huang, Z. Hu and J. Wu, *Macromolecules*, 2003, **36**, 440–448.
70 Y. Chen, G. Nurumbetov, R. Chen, N. Ballard and S. A. F. Bon, *Langmuir*, 2013, **29**, 12657–12662.
71 M. Destribats, V. Lapeyre, M. Wolfs, E. Sellier, F. Leal-Calderon, V. Ravaine and V. Schmitt, *Soft Matter*, 2011, **7**, 7689.
72 W. Richtering, *Langmuir*, 2012, **28**, 17218–17229.
73 A. Šarić and A. Cacciuto, *Soft Matter*, 2013, **9**, 6677–6695.
74 S. Zhang, A. Nelson and P. A. Beales, *Langmuir*, 2012, **28**, 12831–12837.
75 X. Chen, F. Tian, X. Zhang and W. Wang, *Soft Matter*, 2013, **9**, 7592–7600.
76 K. Jaskiewicz, A. Larsen, D. Schaeffel, K. Koynov, I. Lieberwirth, G. Fytas, K. Landfester and A. Kroeger, *ACS Nano*, 2012, **6**, 7254–7262.
77 H. Al-Obaidi, B. Nasseri and A. T. Florence, *J. Drug Targeting*, 2010, **18**, 821–830.
78 A. H. Bahrami, R. Lipowsky and T. R. Weikl, *Phys. Rev. Lett.*, 2012, **109**, 188102.
79 X. Yi, X. Shi and H. Gao, *Phys. Rev. Lett.*, 2011, **107**, 098101.
80 W. T. Góźdź, *Langmuir*, 2007, **23**, 5665–5669.
81 H. Noguchi and M. Takasu, *Biophys. J.*, 2002, **83**, 299–308.
82 S. Cao, G. Wei and J. Z. Y. Chen, *Phys. Rev. E*, 2011, **84**, 050901.
83 M. Dutt, M. J. Nayhouse, O. Kuksenok, S. R. Little and A. C. Balazs, *Curr. Nanosci.*, 2011, **7**, 699–715.
84 S. Lecommandoux, O. Sandre, F. Chécot, J. Rodriguez-Hernandez and R. Perzynski, *Adv. Mater.*, 2005, **17**, 712–718.
85 S. Lecommandoux, O. Sandre, F. Chécot, J. Rodriguez-Hernandez and R. Perzynski, *J. Magn. Magn. Mater.*, 2006, **300**, 71–74.
86 S. Lecommandoux, O. Sandre, F. Chécot and R. Perzynski, *Prog. Solid State Chem.*, 2006, **34**, 171–179.
87 I. Gözen, C. Billerit, P. Dommersnes, A. Jesorkaa and O. Orwar, *Soft Matter*, 2011, **7**, 9706–9713.
88 Y. Natsume, O. Pravaz, H. Yoshidab and M. Imai, *Soft Matter*, 2010, **6**, 5359–5366.
89 M. Paoluzzi, R. Di Leonardo, M. C. Marchetti and L. Angelani, *Sci. Rep.*, 2016, **6**, 34146.
90 I. Koltover, J. O. Rädler and C. R. Safinya, *Phys. Rev. Lett.*, 1999, **82**, 1991–1994.
91 C. Misbah, *J. Phys.: Conf. Ser.*, 2012, **392**, 012005.
92 A. Guckenberger and S. Gekle, *J. Phys.: Condens. Matter*, 2017, **29**, 203001.
93 P. B. Canham, *J. Theor. Biol.*, 1970, **26**, 61–81.
94 E. A. Evans, *Biophys. J.*, 1974, **14**, 923–931.
95 J. Weiner, *Indiana Univ. Math. J.*, 1978, **27**, 19–35.
96 W. Helfrich, *J. Phys.: Condens. Matter*, 1994, **6**, A79–A92.
97 W. Helfrich, *Z. Naturforsch., C: J. Biosci.*, 1973, **28**, 693.
98 U. Seifert, *Adv. Phys.*, 1997, **46**, 13–137.
99 A. Šarić and A. Cacciuto, *Phys. Rev. Lett.*, 2012, **108**, 118101.
100 S. D. Conner and S. L. Schmid, *Nature*, 2003, **422**, 37–44.
101 M. Deserno and W. M. Gelbart, *J. Phys. Chem. B*, 2002, **106**, 5543–5552.
102 K. A. Smith, D. Jasnow and A. C. Balazs, *J. Chem. Phys.*, 2007, **127**, 084703.
103 R. Lipowsky and H.-G. Döbereiner, *Europhys. Lett.*, 1998, **43**, 219–225.
104 O. Le Bihan, P. Bonnafous, L. Marak, T. Bickel, S. Trépout, S. Mornet, F. De Haas, H. Talbot, J.-C. Taveau and O. Lambert, *J. Struct. Biol.*, 2009, **168**, 419–425.
105 K. Jaskiewicz, A. Larsen, A. Kroeger, I. Lieberwirth, K. Koynov, W. Meier, G. Fytas and K. Landfester, *Angew. Chem., Int. Ed.*, 2012, **51**, 4613–4617.
106 P. Nandi, A. Charpilienne and J. Cohen, *J. Virol.*, 1992, **66**, 3363–3367.
107 R. J. Thibault, O. Uzun, R. Hong and V. M. Rotello, *Adv. Mater.*, 2006, **18**, 2179–2183.
108 W. H. Binder, R. Sachsenhofer, D. Farnik and D. Blaas, *Phys. Chem. Chem. Phys.*, 2007, **9**, 6435–6441.
109 H.-Y. Lee, S. H. R. Shin, L. L. Abezgauz, S. A. Lewis, A. M. Chirsan, D. D. Danino and K. J. M. Bishop, *J. Am. Chem. Soc.*, 2013, **135**, 5950–5953.
110 C. Dietrich, M. Angelova and B. Pouligny, *J. Phys. II*, 1997, **7**, 1651–1682.
111 X. Yi and H. Gao, *Langmuir*, 2016, **32**, 13252–13260.
112 S. J. Singer and G. L. Nicolson, *Science*, 1972, **175**, 720–731.

113 R. W. Jaggers, R. Chen and S. A. F. Bon, *Mater. Horiz.*, 2016, **3**, 41–46.
114 L. Paasonen, T. Laaksonen, C. Johans, M. Yliperttula, K. Kontturi and A. Urtti, *J. Controlled Release*, 2007, **122**, 86–93.
115 G. Nurumbetov, N. Ballard and S. A. F. Bon, *Polym. Chem.*, 2012, **3**, 1043–1047.
116 W. J. Duncanson, T. Lin, A. R. Abate, S. Seiffert, R. K. Shah and D. A. Weitz, *Lab Chip*, 2012, **12**, 2135–2145.
117 J. He, Z. Wei, L. Wang, Z. Tomova, T. Babu, C. Wang, X. Han, J. T. Fourkas and Z. Nie, *Angew. Chem., Int. Ed.*, 2013, **52**, 2463–2468.
118 T. Andersen, A. Kyrsting and P. M. Bendix, *Soft Matter*, 2014, **10**, 4268–4274.
119 T. Andersen, A. Bahadori, D. Ott, A. Kyrsting, S. N. S. Reihani and P. M. Bendix, *Nanotechnology*, 2014, **25**, 505101.
120 G. Wu, A. Mikhailovsky, H. A. Khant, C. Fu, W. Chiu and J. A. Zasadzinski, *J. Am. Chem. Soc.*, 2008, **130**, 8175–8177.
121 A. Kyrsting, P. M. Bendix, D. G. Stamou and L. B. Oddershede, *Nano Lett.*, 2011, **11**, 888–892.
122 A. S. Urban, M. Fedoruk, M. R. Horton, J. O. Rädler, F. D. Stefani and J. Feldmann, *Nano Lett.*, 2009, **9**, 2903–2908.
123 P. M. Bendix, S. N. S. Reihani and L. B. Oddershede, *ACS Nano*, 2010, **4**, 2256–2262.
124 P. M. Bendix, L. Jauffred, K. Norregaard and L. B. Oddershede, *IEEE J. Sel. Top. Quantum Electron.*, 2014, **20**, 15–26.
125 R. M. Gorgoll, T. Tsubota, K. Harano and E. Nakamura, *J. Am. Chem. Soc.*, 2015, **137**, 7568–7571.
126 E. Amstad, J. Kohlbrecher, E. Müller, T. Schweizer, M. Textor and E. Reimhult, *Nano Lett.*, 2011, **11**, 1664–1670.
127 Y. Chen, A. Bose and G. D. Bothun, *ACS Nano*, 2010, **4**, 3215–3221.
128 S. Ma, D. Qi, M. Xiao and R. Wang, *Soft Matter*, 2014, **10**, 9090–9097.
129 Y. Mai and A. Eisenberg, *J. Am. Chem. Soc.*, 2010, **132**, 10078–10084.
130 J. K. Sigurdsson and P. J. Atzberger, *Soft Matter*, 2016, **12**, 6685–6707.
131 S.-H. Park, S.-G. Oh, J.-Y. Mun and S.-S. Han, *Colloids Surf., B*, 2005, **44**, 117–122.
132 S.-H. Park, S.-G. Oh, J.-Y. Mun and S.-S. Han, *Colloids Surf., B*, 2006, **48**, 112–118.
133 L. Wang, Y. Liu, J. He, M. J. Hourwitz, Y. Yang, J. T. Fourkas, X. Han and Z. Nie, *Small*, 2015, **11**, 3762–3767.
134 F. Peng, Y. Tu, J. C. M. van Hest and D. A. Wilson, *Angew. Chem.*, 2015, **127**, 11828–11831.
135 B. Herranz-Blanco, L. R. Arriaga, E. Mäkilä, A. Correia, N. Shrestha, S. Mirza, D. A. Weitz, J. Salonen, J. Hirvonen and H. A. Santos, *Lab Chip*, 2014, **14**, 1083–1086.
136 C. Sanson, O. Diou, J. Thévenot, E. Ibarboure, A. Soum, A. Brûlet, S. Miraux, E. Thiaudière, S. Tan, A. Brisson, V. Dupuis, O. Sandre and S. Lecommandoux, *ACS Nano*, 2011, **5**, 1122–1140.
137 G. Béalle, L. Lartigue, C. Wilhelm, J. Ravaux, F. Gazeau, R. Podor, D. Carrière and C. Ménager, *Phys. Chem. Chem. Phys.*, 2014, **16**, 4077–4081.
138 S. Nappini, M. Bonini, F. B. Bombelli, F. Pineider, C. Sangregorio, P. Baglioni and B. Nordèn, *Soft Matter*, 2011, **7**, 1025–1037.
139 S. Nappini, M. Bonini, F. Ridi and P. Baglioni, *Soft Matter*, 2011, **7**, 4801–4811.
140 X. Ding, K. Cai, Z. Luo, J. Li, Y. Hu and X. Shen, *Nanoscale*, 2012, **4**, 6289–6292.
141 S. Nappini, T. Al Kayal, D. Berti, B. Nordèn and P. Baglioni, *J. Phys. Chem. Lett.*, 2011, **2**, 713–718.
142 D. A. Wilson, R. J. M. Nolte and J. C. M. van Hest, *Nat. Chem.*, 2012, **4**, 268–274.
143 S. El Andaloussi, I. Mäger, X. O. Breakefield and M. J. A. Wood, *Nat. Rev. Drug Discovery*, 2013, **12**, 347–357.
144 R. F. Ismagilov, A. Schwartz, N. Bowden and G. M. Whitesides, *Angew. Chem., Int. Ed.*, 2002, **114**, 674–676.
145 Y. Tu, F. Peng, X. Sui, Y. Men, P. B. White, J. C. M. van Hest and D. A. Wilson, *Nat. Chem.*, 2017, **9**, 480–486.
146 A. Joseph, C. Contini, D. Cecchin, S. Nyberg, L. Ruiz-Perez, J. Gaitzsch, G. Fullstone, X. Tian, J. Azizi, J. Preston, G. Volpe and G. Battaglia, *Sci. Adv.*, 2017, **3**, e1700362.

